

Supplementary Materials for

Molecular parallelism in fast-twitch muscle proteins in echolocating mammals

Jun-Hoe Lee, Kevin M. Lewis, Timothy W. Moural, Bogdan Kirilenko, Barbara Borgonovo, Gisa Prange, Manfred Koessl, Stefan Huggenberger, ChulHee Kang, Michael Hiller*

*Corresponding author. Email: hiller@mpi-cbg.de

Published 26 September 2018, *Sci. Adv.* **4**, eaat9660 (2018)
DOI: 10.1126/sciadv.aat9660

This PDF file includes:

- Fig. S1. Computational approach to identify parallel amino acid substitutions between pairs of independent lineages.
- Fig. S2. Phylogeny of the 30 placental mammals.
- Fig. S3. Radical parallel substitutions in conserved positions between microbat and dolphin in hearing-related genes.
- Fig. S4. Convergence of microbat and dolphin Myh2 toward Myh4.
- Fig. S5. *Myh4* is deleted in the cetacean lineage.
- Fig. S6. Unassembled genomic and RNA reads confirm the absence of *Myh4* in the cetacean lineage.
- Fig. S7. The amount of aligning intronic sequence distinguishes *Myh* orthologs from paralogs.
- Table S1. Classification of all parallel amino acid substitutions detected by reconstructing ancestral sequences with a maximum likelihood and a Bayesian approach.
- Table S2. Functional enrichments of proteins with parallel substitutions between the microbat (little brown bat) and the bottlenose dolphin.
- Table S3. Pairs of independent branches and their number of parallel substitutions in fast-twitch versus slow-twitch fiber proteins.
- Table S4. GC-biased gene conversion alone can potentially explain only one of the seven parallel substitutions in the fast-twitch muscle proteins.
- Table S5. Top 30 genes with a significantly higher expression level in the anterior cricothyroid muscle compared to breast muscle of *P. parnellii*.
- Table S6. Expression of calsequestrin, Ca²⁺ ATPase, myosin heavy chain, and myosin light chain genes in the anterior cricothyroid muscle and the breast muscle of the echolocating *P. parnellii* bat.
- References (49–55)

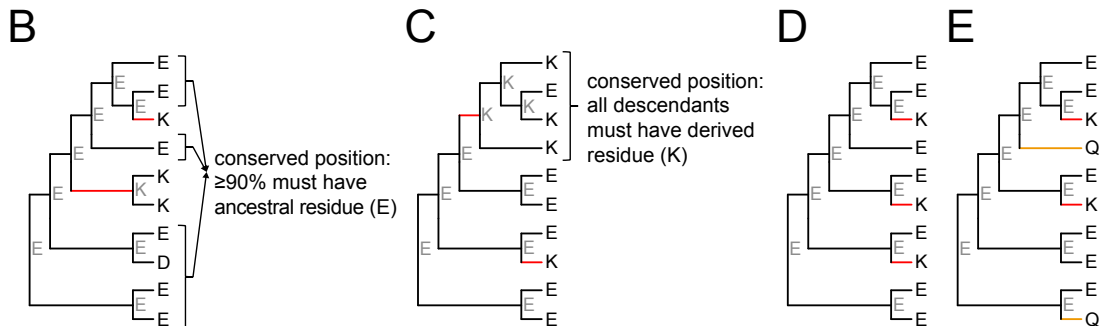
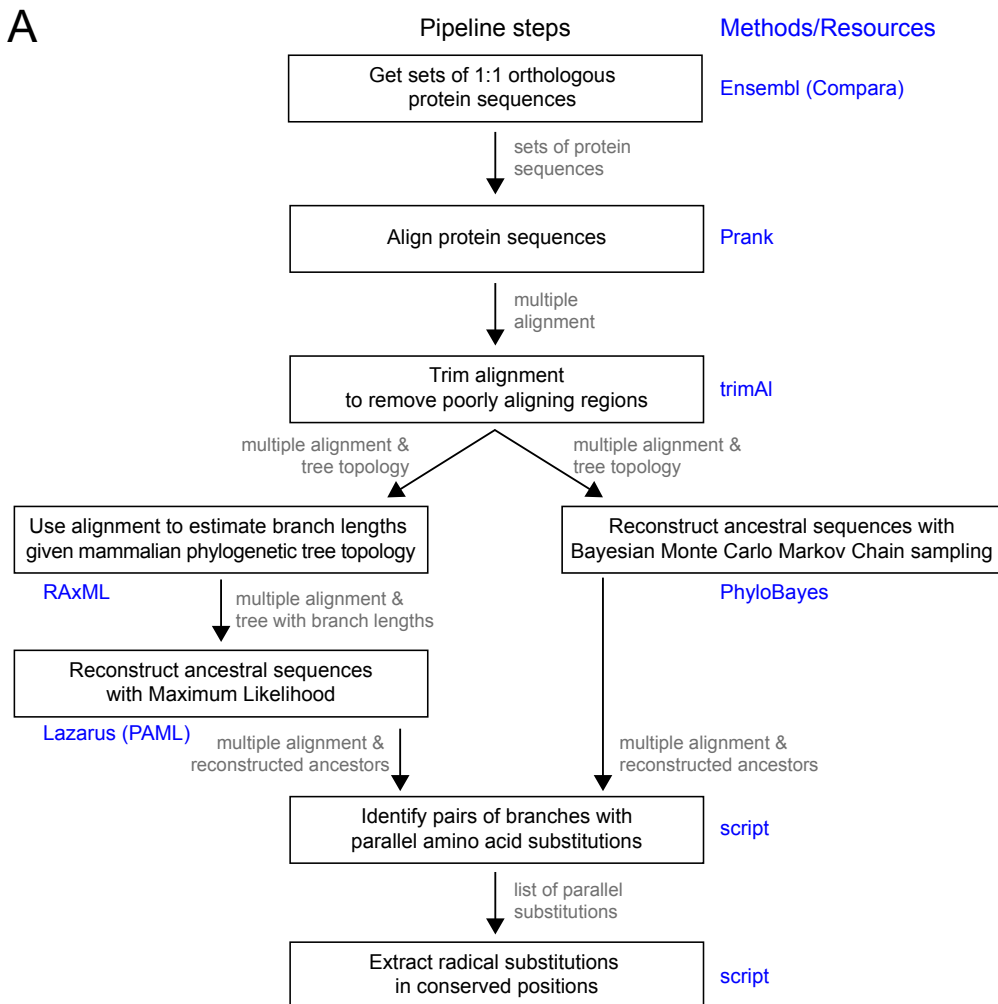


Fig. S1. Computational approach to identify parallel amino acid substitutions between pairs of independent lineages.

(A) Overview of the step-by-step analyses to detect radical parallel amino acid substitutions in conserved positions. The methods section provides a detailed description of each step including the parameters we used.

(B-E) Illustration of ancestral sequence reconstruction to infer parallel substitutions and assessing whether they occur in a conserved position. For clarity, these schematic examples include only 10 species.

(B) For a parallel substitution in a conserved position, we required that at least 90% of the species outside of the two convergent lineages have the ancestral amino acid (E in this case).

- (C) For a parallel substitution in a conserved position, we required that all species that descend from both branches share the derived amino acid (K). Due to a reversal to the ancestral amino acid (E) in one species descending from the first branch, this condition is not fulfilled in the illustrated case.
- (D) A parallel amino acid substitution can occur on more than two branches. In this case, our method would identify three branch pairs with the same parallel substitution.
- (E) Two different parallel amino acid substitutions can occur at the same position ($E \rightarrow K$ and $E \rightarrow Q$). In this case, our method would identify two branch pairs (red and orange), each with a different parallel substitution.

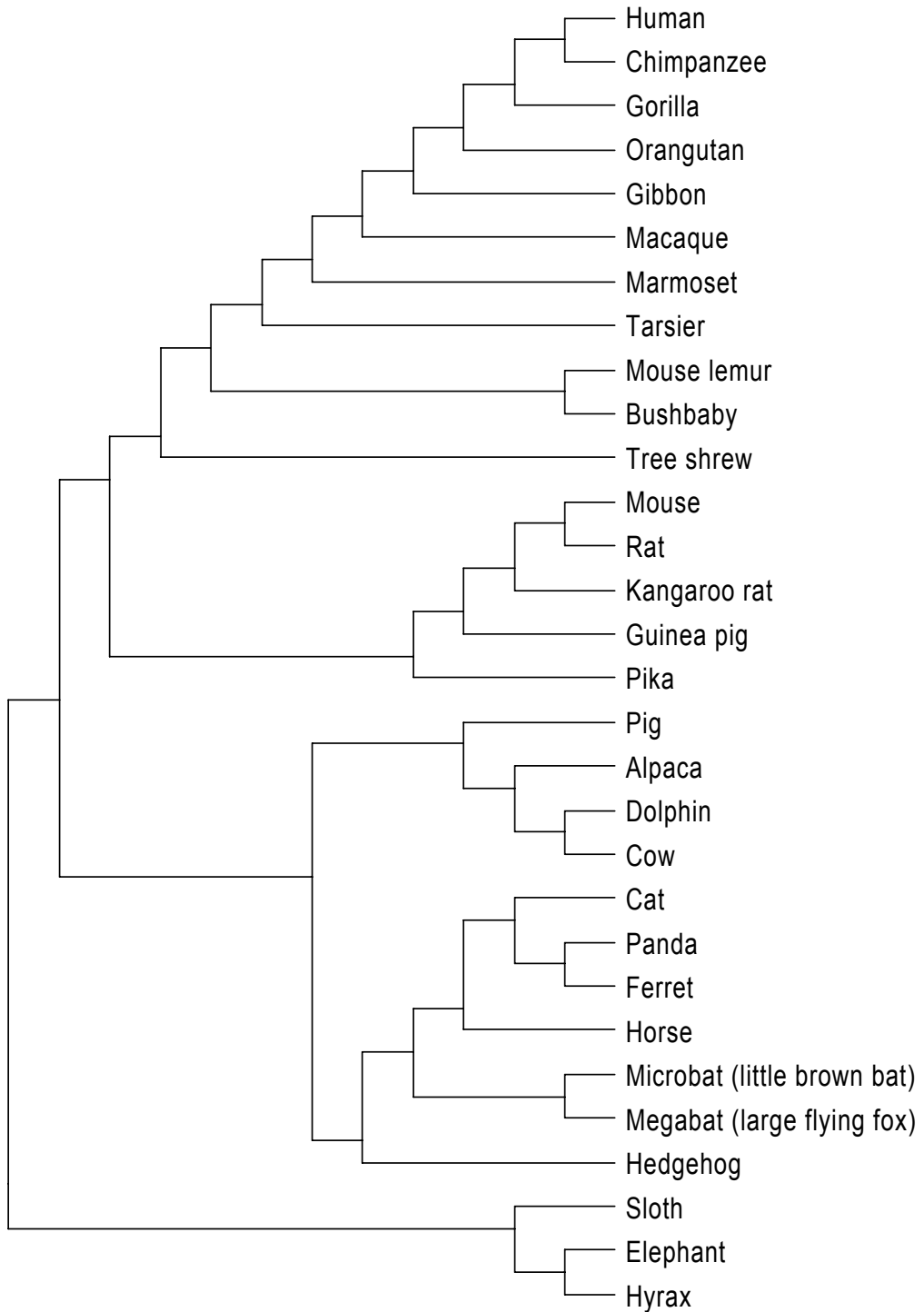


Fig. S2. Phylogeny of the 30 placental mammals.

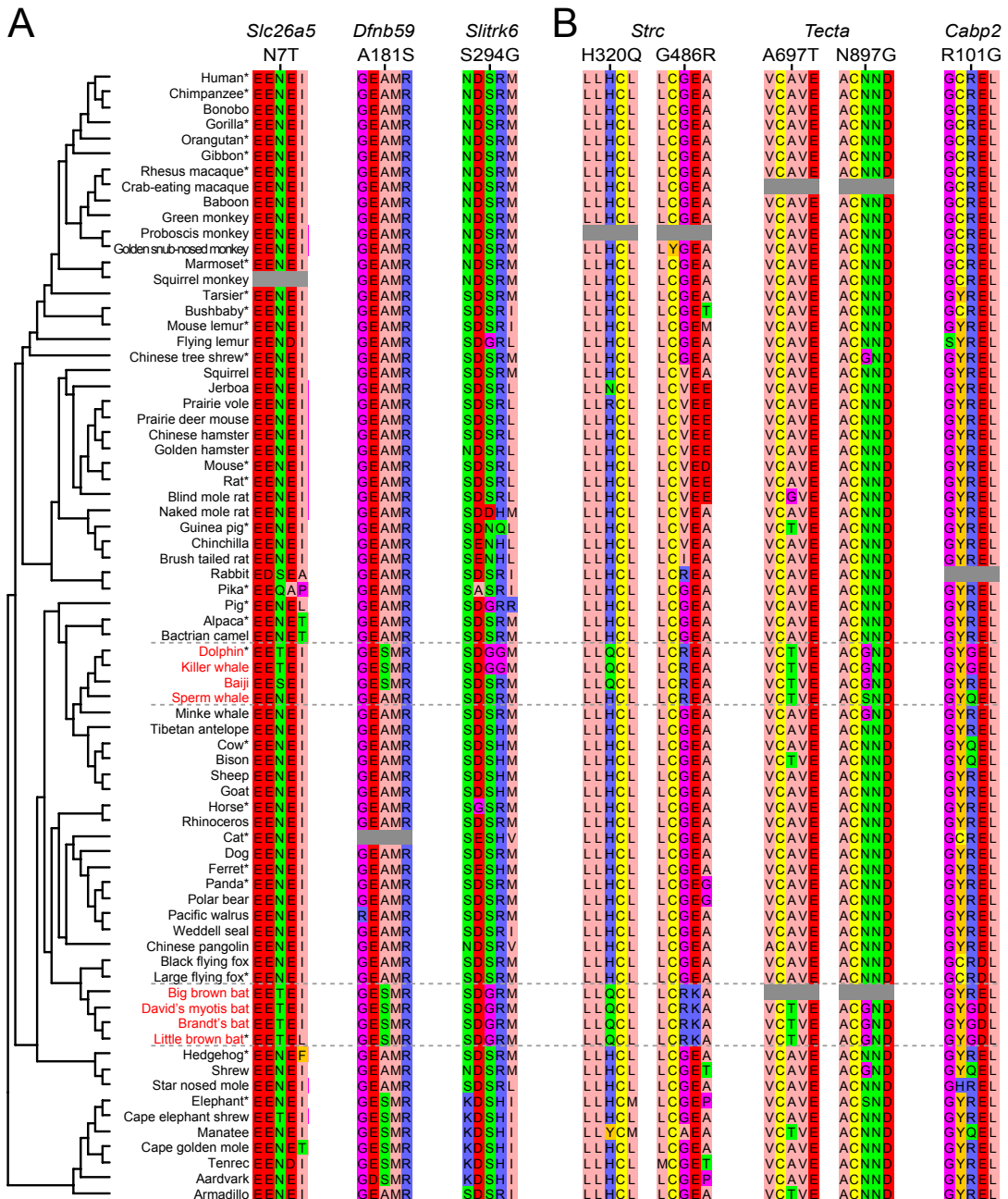


Fig. S3. Radical parallel substitutions in conserved positions between microbat and dolphin in hearing-related genes.

(A) The parallel substitutions in Prestin (*Slc26a5*) (8, 9), Dfnb59 (10) and Slitrk6 (4) have already been described. Note that the non-echolocating cape elephant shrew also exhibits the N7T mutation that was associated with functional changes in Prestin. In addition, the P26L substitution that was also experimentally shown to affect Prestin function (49) also occurs in the non-echolocating cat and the minke whale (not shown).

(B) Parallel substitutions in the hearing-related proteins stereocilin (*Strc*), tectorin alpha (*Tecta*) and calcium binding protein 2 (*Cabp2*) are described here for the first time to the best of our knowledge. Mutations in all three genes are associated with hearing impairments and deafness (16, 50, 51).

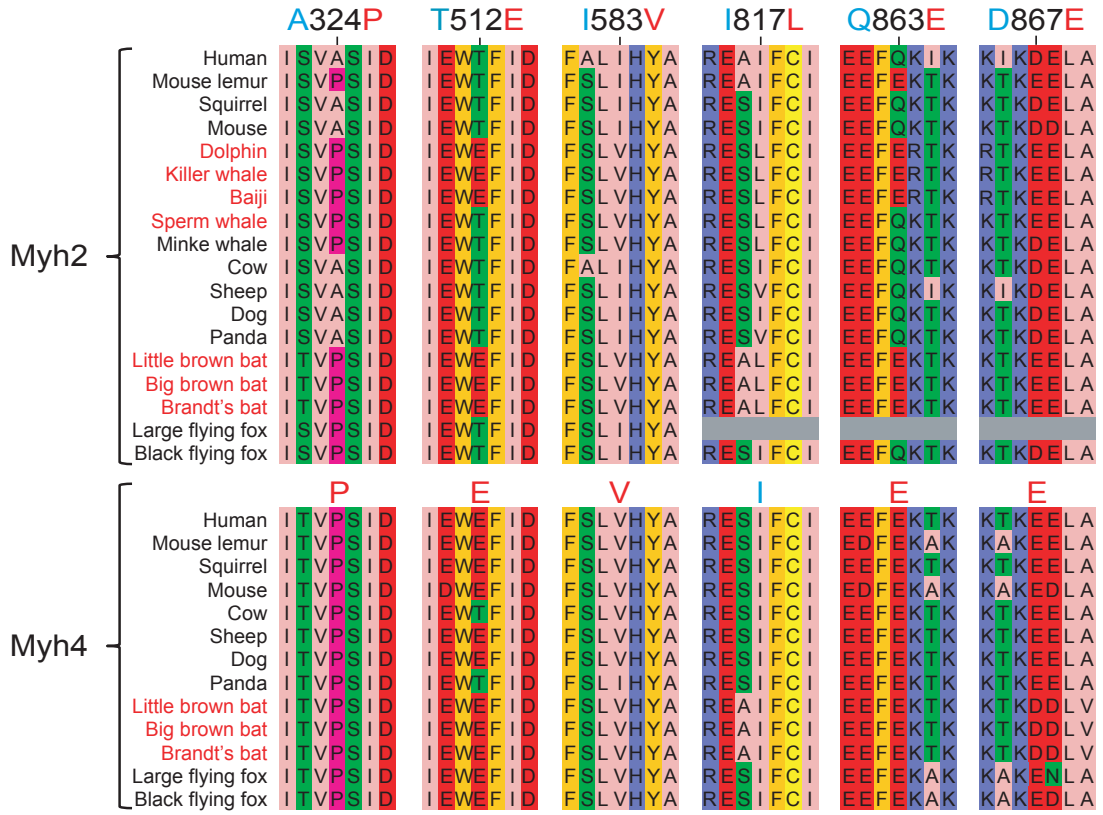


Fig. S4. Convergence of microbat and dolphin Myh2 toward Myh4.

The derived amino acids of the Myh2 substitutions T512E and Q863E (described in the main text) occur in Myh4 in most mammals. Amino acids that are ancestral in Myh2 are in light blue, derived amino acids are in red.

Fibers expressing Myh4 have the highest shortening velocity (23). In addition to T512E and Q863E, four other parallel substitutions are shown that were not classified as radical or occurred at an alignment position that was not classified as conserved. The A324P substitution is noteworthy because it is located directly next to a serine (S325) that is close to the nucleotide binding pocket and is involved in binding phosphate (52, 53). Together, for five of these six parallel substitutions in microbat and dolphin Myh2, the derived residue also occurs in Myh4, suggesting that microbat and dolphin Myh2 converged towards a higher similarity with Myh4.

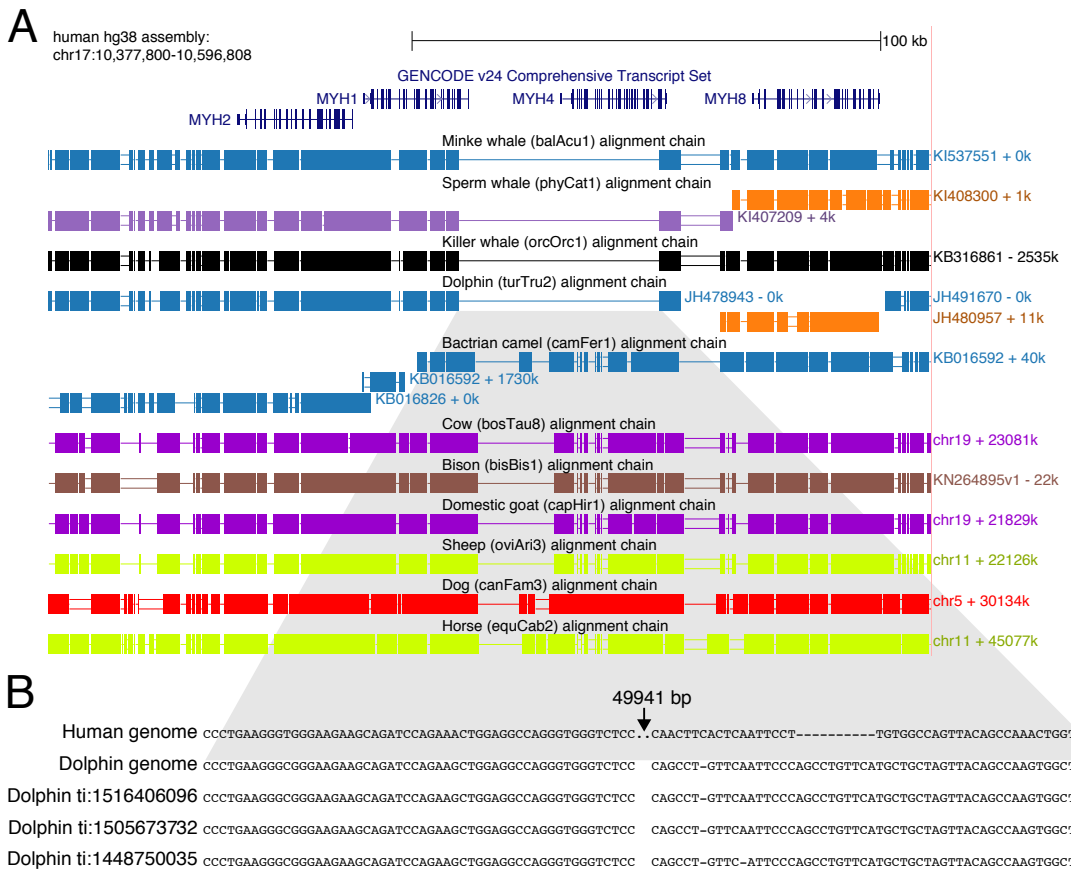


Fig. S5. *Myh4* is deleted in the cetacean lineage.

(A) UCSC genome browser (54) screenshot showing the *MYH2/1/4/8* gene cluster in the human hg38 genome assembly. The alignment chains show pairwise genome alignments between human and other mammals. Aligning regions are shown as blocks. Although *MYH4* aligns to other species, all four cetacean species share the same deletion (single line) that spans *MYH4*, suggesting that this deletion occurred in the ancestor of toothed and baleen whales. Some assemblies such as sperm whale, dolphin and camel have several scaffolds that align to this locus, shown by separate chains. For clarity, only orthologous alignment chains are shown.

(B) Alignment of the human genomic sequence that spans the deletion breakpoint (grey highlight) to the dolphin genome. The deletion breakpoint in the dolphin genome is confirmed by unassembled (raw) Sanger sequencing reads stored in the NCBI trace archive.

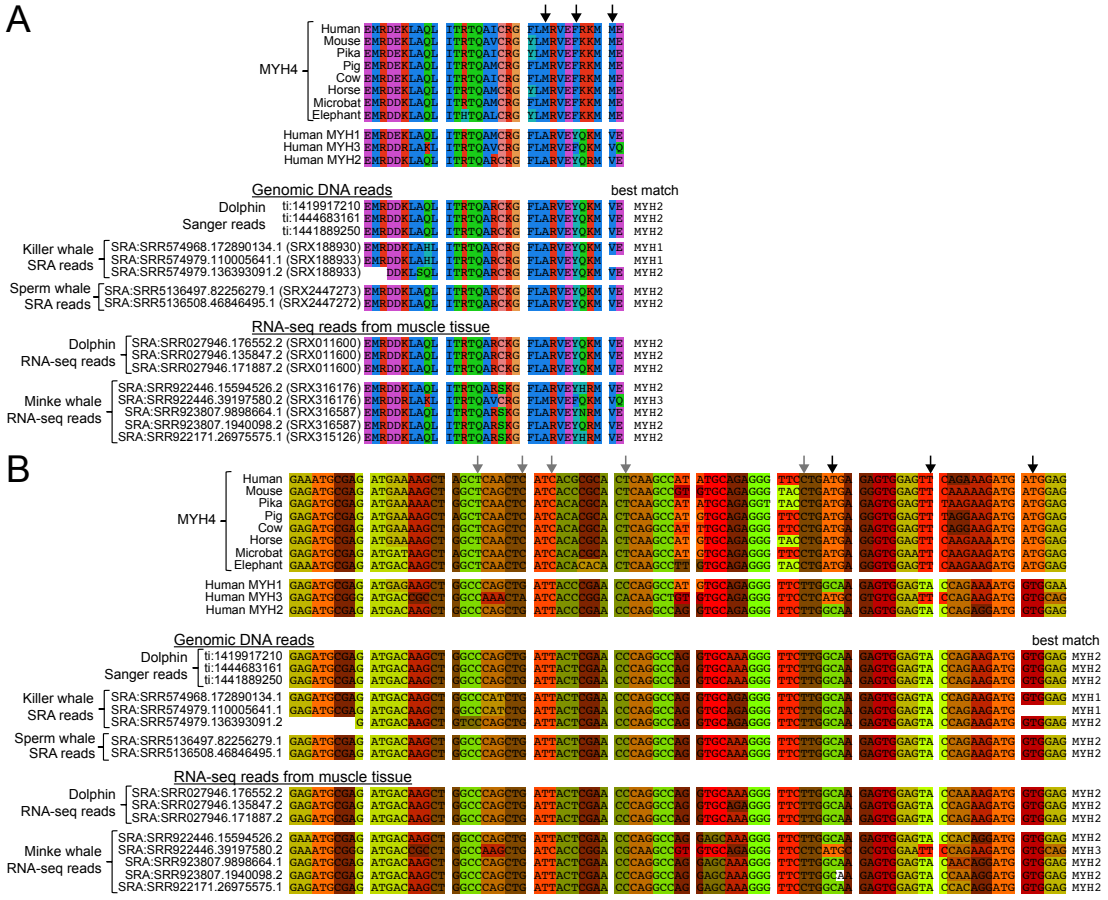


Fig. S6. Unassembled genomic and RNA reads confirm the absence of Myh4 in the cetacean lineage.

(A) Since Myh proteins are very similar to each other, we selected a Myh4 region with several unique amino acid changes that are conserved among the Myh4 orthologs, but are not found in Myh1 and Myh2 (black arrows). For comparison, the sequences of MYH1/2/3 are also shown. We used *MYH4* DNA sequences (panel B) as a “bait” and searched Sanger reads from the NCBI trace archive (dolphin) and Illumina reads from the Sequence Read Archive (SRA) (killer and sperm whale) to retrieve a putative Myh4 sequence. We also searched available RNA-seq datasets from muscle tissue for dolphin and minke whale. None of these searches retrieved *Myh4* in any cetacean species. Instead, the hits we retrieved belong to other *Myh* genes (often *Myh2*), as determined by amino acids that characterize other *Myh* genes (shown by translated protein sequences in this panel) and by mapping the retrieved sequence back to the genome. Similar results were obtained when using different Myh4 regions as baits (not shown). Only a few representative reads are shown for space considerations.

(B) The same data as in panel A, with the DNA sequences shown instead. Grey arrows highlight further synonymous differences between *Myh4* and *Myh1/2*. In summary, raw RNA or DNA sequencing reads corroborate that *Myh4* is deleted in the cetacean lineage.

Data:

- SRX316587, SRX316176, SRX315126: Minke whale muscle transcriptome data (Illumina HiSeq2000)
- SRX011600: Dolphin muscle transcriptome data (454 sequencing)
- SRX2447272, SRX2447273: Sperm whale genomic DNA (Illumina HiSeq X Ten)
- SRX188933, SRX188930: Killer whale genomic DNA (Illumina HiSeq 2000)
- Trace identifiers of the dolphin Sanger sequencing reads are given next to the read.

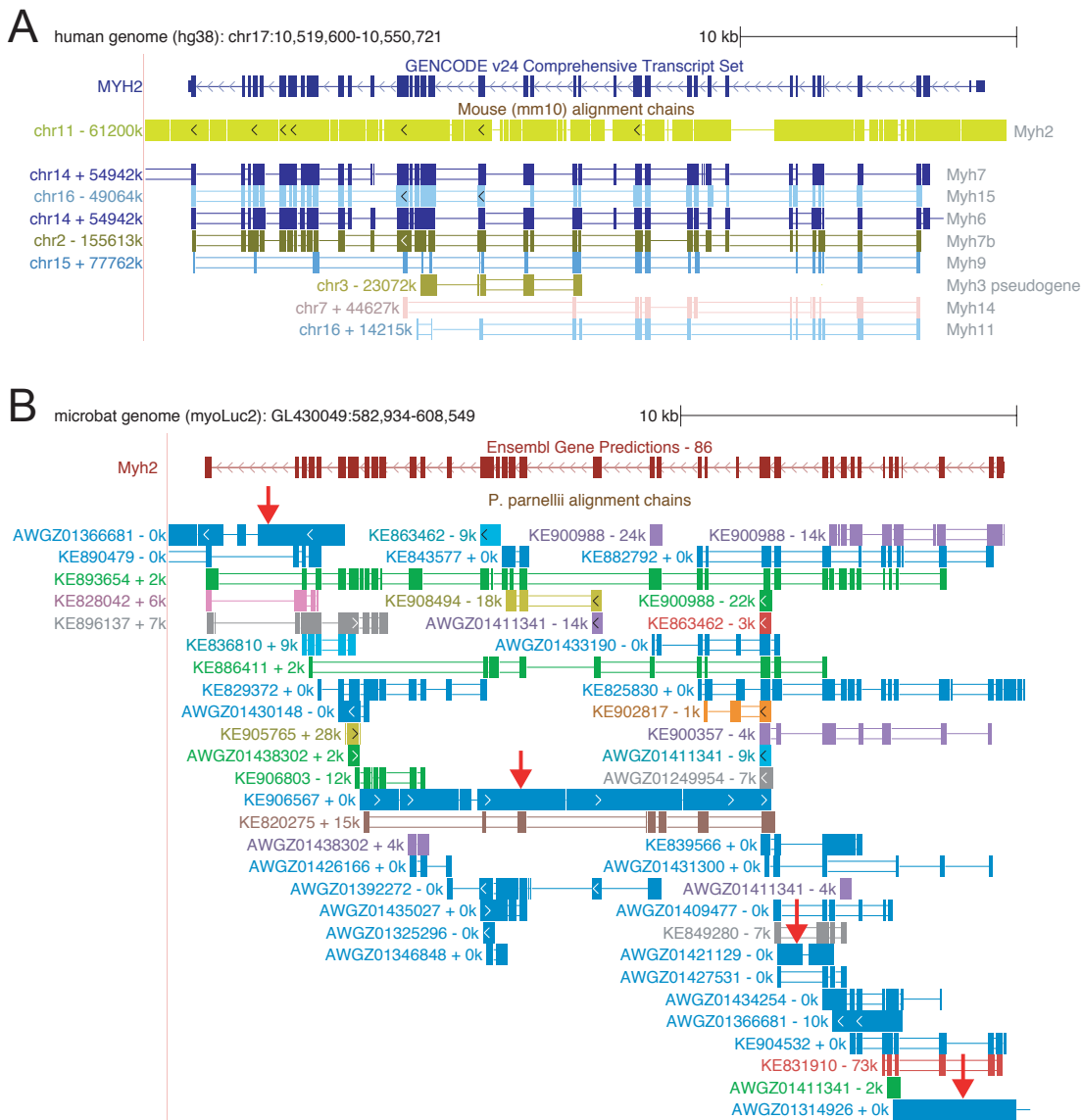


Fig. S7. The amount of aligning intronic sequence distinguishes *Myh* orthologs from paralogs.

(A) Alignment chains between the well-annotated human and mouse genome show that intronic sequences align well between *Myh* orthologs but not paralogs. The top-level chain aligns both exons and introns of human *MYH2* and corresponds to the mouse locus encoding the *Mhy2* ortholog. In contrast, all other chains that align mostly conserved exonic sequence correspond to paralogs or pseudogenes, as annotated on the right.

(B) Alignment chains between the microbat *Myh2* locus and the *P. parnellii* genome. By selecting the chains that align intronic sequence (red arrows), we obtained the *P. parnellii* loci that most likely encode the *Myh2* ortholog. This allowed us to manually assemble the *P. parnellii* *Myh2* transcript. Note that the orthologous *Myh2* loci are located on separate contigs because of the fragmentation of the *P. parnellii* genome. Since alignment chains cannot span different contigs, these orthologous loci are indicated by separate alignment chains.

Table S1. Classification of all parallel amino acid substitutions detected by reconstructing ancestral sequences with a Maximum Likelihood and a Bayesian approach.

Maximum Likelihood ancestral reconstruction	# parallel substitutions	percent
not radical, non-conserved position	542,457	39.8%
radical, non-conserved position	474,013	34.8%
not radical, conserved position	199,627	14.7%
radical, conserved position	145,482	10.7%
total	1,361,579	100%

Bayesian ancestral reconstruction		
not radical, non-conserved position	568,593	39.9%
radical, non-conserved position	522,812	36.7%
not radical, conserved position	193,746	13.6%
radical, conserved position	140,542	9.9%
total	1,425,693	100%

Table S2. Functional enrichments of proteins with parallel substitutions between the microbat (little brown bat) and the bottlenose dolphin.

(A) Functional enrichments of 409 proteins, where Maximum Likelihood ancestral reconstruction infers parallel substitutions.

(B) Functional enrichments of 416 proteins, where Bayesian ancestral reconstruction infers parallel substitutions.

GeneTrail2 (version 1.5 (55)) enrichment results are shown with an adjusted P-value cutoff of 0.05. Only the top 15 enrichments are shown for GO Biological Process (151 significant enrichments in A, 160 enrichments in B). Enriched terms relating to calcium ion transport and muscle fiber components are in red font.

A Maximum Likelihood ancestral reconstruction

Name	Number of hits	Expected score	Adjusted p-value
GO_-_Biological_Process			
carbohydrate transport(5)	12	1.12	1.04E-004
cellular response to acid chemical(5)	12	1.11	1.04E-004
epithelial tube morphogenesis(5)	15	2.04	1.04E-004
cell projection assembly(5)	15	2.26	2.96E-004
RNA localization(4)	11	1.16	5.19E-004
cellular response to heat(5)	9	0.67	5.19E-004
multicellular organism growth(4)	10	0.99	1.05E-003
establishment or maintenance of cell polarity(4)	10	1.01	1.09E-003
Golgi vesicle transport(6)	12	1.85	1.99E-003
calcium ion transmembrane transport(8)	10	1.21	1.99E-003
cell cycle phase(3)&mitotic cell cycle phase(4)	12	1.87	1.99E-003
cellular response to retinoic acid(6)	7	0.44	1.99E-003
columnar cuboidal epithelial cell differentiation(7)	9	0.85	1.99E-003
establishment of cell polarity(5)	8	0.66	1.99E-003
hexose transport(7)	9	0.89	1.99E-003
GO_-_Molecular_Function			
helicase activity(8)	12	0.98	1.09E-005
protein C terminus binding(4)	11	1.14	2.75E-004
calcium ion transmembrane transporter activity(9)	9	0.77	4.31E-004
cation channel activity(7)	13	1.91	4.31E-004
nucleocytoplasmic transporter activity(3)	5	0.09	4.31E-004
calcium channel activity(8)	8	0.69	1.75E-003
divalent inorganic cation transmembrane transporter activity(8)	9	1.00	2.44E-003
calmodulin binding(4)	9	1.09	4.05E-003
purine NTP dependent helicase activity(9)&ATP dependent helicase activity(10)	7	0.63	7.92E-003
SMAD binding(4)	6	0.47	1.53E-002
DNA helicase activity(9)	5	0.33	3.53E-002
amino acid binding(6)	6	0.57	3.53E-002
motor activity(8)	7	0.89	4.11E-002
thyroid hormone receptor binding(5)	4	0.17	4.11E-002
nuclear hormone receptor binding(6)	7	0.93	4.98E-002
KEGG_-_Pathways			
Calcium signaling pathway	9	1.09	4.59E-003
RNA transport	8	1.01	1.11E-002

B Bayesian ancestral reconstruction

Name	Number of hits	Expected score	Adjusted p-value
GO_-_Biological_Process			
cellular response to acid chemical(5)	12	1.12	1.91E-004
epithelial tube morphogenesis(5)	15	2.07	1.91E-004
carbohydrate transport(5)	11	1.14	4.22E-004
cell projection assembly(5)	15	2.30	4.22E-004
membrane disassembly(5)&nuclear envelope disassembly(6)	7	0.29	4.22E-004
mitotic nuclear envelope disassembly(6)	7	0.28	4.22E-004
nuclear envelope organization(5)	8	0.48	5.75E-004
cell cycle phase(3)&mitotic cell cycle phase(4)	13	1.90	8.94E-004
biological phase(2)	13	1.94	9.12E-004
establishment or maintenance of cell polarity(4)	10	1.03	9.12E-004
multicellular organism growth(4)	10	1.01	9.12E-004
columnar cuboidal epithelial cell differentiation(7)	9	0.87	1.87E-003
positive regulation of cytosolic calcium ion concentration(11)	11	1.45	1.87E-003
prophase(4)&mitotic prophase(5)	7	0.42	1.87E-003
RNA localization(4)	10	1.18	1.97E-003
GO_-_Molecular_Function			
helicase activity(8)	11	0.99	1.50E-004
calcium ion transmembrane transporter activity(9)	9	0.79	6.12E-004
cation channel activity(7)	13	1.95	6.12E-004
nucleocytoplasmic transporter activity(3)	5	0.09	6.12E-004
protein C terminus binding(4)	10	1.16	1.19E-003
calcium channel activity(8)	8	0.70	1.96E-003
divalent inorganic cation transmembrane transporter activity(8)	9	1.02	2.76E-003
calmodulin binding(4)	9	1.11	4.58E-003
SMAD binding(4)	6	0.48	1.85E-002
DNA helicase activity(9)	5	0.34	4.19E-002
amino acid binding(6)	6	0.58	4.19E-002
KEGG_-_Pathways			
Calcium signaling pathway	9	1.11	2.60E-003
Lysosome	8	0.77	2.60E-003

Table S3. Pairs of independent branches and their number of parallel substitutions in fast-twitch versus slow-twitch fiber proteins.

The table is sorted by the difference of the number of radical parallel substitutions in conserved positions observed in fast- vs. slow-twitch fiber proteins. The top and bottom 20 branch pairs are shown. None of the 1,295 other branch pairs have a greater difference (maximum is 4 for horse-pig and megabat-panda and Bayesian reconstruction) than the pair of microbat (little brown bat) and bottlenose dolphin with a difference of 7. Results for Maximum Likelihood ancestral reconstruction is shown on the left, Bayesian ancestral reconstruction is shown on the right.

Maximum Likelihood ancestral reconstruction			Bayesian ancestral reconstruction		
branch pair	# radical parallel substitutions in conserved positions in		branch pair	# radical parallel substitutions in conserved positions in	
	fast-twitch fiber proteins	slow-twitch fiber proteins		fast-twitch fiber proteins	slow-twitch fiber proteins
		fast – slow			fast – slow
Microbat,Dolphin	7	0	Microbat,Dolphin	7	0
Horse,Pig	3	0	Horse,Pig	4	0
Megabat,Panda	3	0	Megabat,Panda	4	0
Mouse_Imur-Bushbaby,Tarsier	3	0	Microbat,Panda	3	0
Cat,Pig	2	0	Mouse_Imur-Bushbaby,Tarsier	3	0
Cow,Pika	2	0	Cat,Pig	2	0
Elephant,Orangutan	2	0	Cow,Pika	2	0
Elephant,Panda	4	2	Ferret,Guinea_pig	2	0
Elephant,Pig	2	0	Guinea_pig,Gibbon	2	0
Ferret,Guinea_pig	2	0	Horse,Ferret	2	0
Guinea_pig,Gibbon	2	0	Horse,Mouse-Rat	2	0
Horse,Mouse-Rat	2	0	Horse,Panda	2	0
Horse,Panda	2	0	Megabat,Dolphin	2	0
Microbat,Ferret	2	0	Microbat,Ferret	2	0
Microbat,Panda	2	0	Microbat-Megabat,Mouse-Rat	2	0
Microbat-Megabat,Mouse-Rat	2	0	Mouse-Rat,Tarsier	3	1
Panda,Bushbaby	2	0	Panda,Bushbaby	2	0
Panda,Orangutan	2	0	Panda,Orangutan	2	0
Panda,Pika	2	0	Panda,Pika	2	0
Pig-Cat,Guinea_pig	2	0	Pig-Cat,Guinea_pig	2	0
...			...		
Elephant,Human-Orangutan	0	2	Sloth,Marmoset	0	1
Horse,Human-Orangutan	0	2	Cow,Kangaroo_rat	0	2
Hyrax,Kangaroo_rat	0	2	Cow,Tree_shrew	0	2
Hyrax,Mouse-Rat	0	2	Horse,Human-Orangutan	0	2
Kangaroo_rat,Bushbaby	0	2	Hyrax,Kangaroo_rat	0	2
Megabat,Kangaroo_rat	0	2	Kangaroo_rat,Bushbaby	0	2
Megabat,Mouse-Rat	0	2	Megabat,Kangaroo_rat	0	2
Megabat,Pika	0	2	Megabat,Mouse-Rat	0	2
Pig,Bushbaby	0	2	Megabat,Pika	0	2
Pig,Guinea_pig	0	2	Pig,Bushbaby	0	2
Pika,Bushbaby	0	2	Pig,Guinea_pig	0	2
Pika,Guinea_pig	0	2	Pika,Bushbaby	0	2
Pika,Mouse	0	2	Pika,Guinea_pig	0	2
Sloth,Marmoset	0	2	Pika,Mouse	0	2
Tree_shrew,Bushbaby	0	2	Tree_shrew,Bushbaby	0	2
Cat,Bushbaby	0	3	Cat,Bushbaby	0	3
Megabat,Cow	0	3	Megabat,Cow	0	3
Dolphin,Human-Marmoset	0	4	Dolphin,Human-Marmoset	0	4
Guinea_pig,Bushbaby	1	7	Guinea_pig,Bushbaby	1	7
Gibbon,Chimpanzee	0	12	Gibbon,Chimpanzee	0	12
		-12			-12

Table S4. GC-biased gene conversion alone can potentially explain only one of the seven parallel substitutions in the fast-twitch muscle proteins.

The codon regions of the parallel substitution sites (bold font) in *Casq1*, *Atp2a1*, *Myh2* and *Myl1* are shown. G/C → A/T (strong to weak) substitutions are shown in green, G/C → C/G and A/T → T/A (strong to strong or weak to weak) substitutions are shown in blue, and A/T → G/C (weak to strong) substitutions are shown in red font. A/T → G/C substitutions could potentially be the result of GC-biased gene conversion. Note that only K49Q in *Myl1*, which involves a single A → C change, could potentially be attributed to GC-biased gene conversion alone. The T512E in *Myh2* involves two nucleotide changes (A→G and C→A). Overall, 8 of the 17 substitutions are G/C → A/T and only 4 substitutions are A/T → G/C, suggesting that GC-biased gene conversion is not a major factor explaining these seven parallel amino acid substitutions.

Gene	Parallel substitution	Species	Amino acid sequence		Nucleotide sequence	Nucleotide substitution	
			sequence				
CASQ1	E35Q	Human	VQGQEGL	GTACAGGGCAGGAAGGGCTG			
		Mouse	VQGEDGL	GTCCAGGGGAAAGATGGGTTG			
		Pig	VHGEEGL	GTGCACGGGAGGAAGGGCTG			
		Dolphin	VGRQDGL	GTGCAGAGGCAAGACGGCTG	G → C , G → A		
		Cow	VQGE EGL	GTGCAGGGGAGGAAGGGCTC			
		Horse	VQGEEGL	GTGCAGGGGAGGAAGGGCTG			
		Megabat	VQGEDGL	GTCCAAGGGAGGATGGCTG	G → C		
		Microbat	VRGQDGL	GTGCAGGGCAGGACGGCTG	G → C		
ATP2A1	E381K	Human	EKDAAVA	GAGAAGGATGCACTGTGGCC			
		Mouse	EKDAAVA	GAGAAGGATGCACTGTGGCC			
		Pig	EKDAAVA	GAGAAGGACCGCGGCCGTAGCC			
		Dolphin	EKD TAVA	GAGAAGGACACGGCTGTAGCC	G → A		
		Cow	EKDAAVA	GAGAAGGACCGCGGCCGTAGCC			
		Horse	EKDAAVA	GAGAAGGATGCACTGTAGCC			
		Megabat	EKDAAVA	GAGAAGGATGCACTGTAGCC			
		Microbat	EKD TAVA	GAGAAGGACACAGCTGTAGCC	G → A		
MYH2	T512E	Human	PVELIEG	CCTGTGGAATTGATTGAGGT			
		Mouse	PVELIEG	CCTGTAGAGGTTGATTGAGGT			
		Pig	PVELIEG	CCTGTGGAACTGATTGAGGG			
		Dolphin	PVEFIEG	CCTGTGGAATTATTGAGGGT	G → T		
		Cow	PVELIEG	CCTGTGGAATTGATTGAGGGT			
		Horse	PVELIEG	CCTGTAGAATTGATTGAGGGT			
		Megabat	PVELIEG	CCTGTGGAATTGATTGAGGGT			
		Microbat	PVEFIEG	CCTGTGGAATTATTGAGGGT	G → C		
Q863E	Q863E	Human	EEFQKIK	GAAGAATTTCAGAAAATAAA			
		Mouse	EEFQKTK	GAGGAGTCCAGAAAACAAA			
		Pig	EEFQKTK	GAGGAGTCCAGAAAACCAA			
		Dolphin	EEFERTK	GAAGAGTTGAGAGAACTAAA	C → G		
		Cow	EEFQKTK	GAAGAGTTCCAGAAAACAAA			
		Horse	EEFQKTK	GAGGAGTTCCAGAAAACAAA			
		Black flying fox	EEFQKTK	GAAGAATTTCAGAAAACAAA			
		Microbat	EEFEKTK	GAAGAGTTGAGAGACCAAA	C → G		
MYL1	K49Q	Human	EFSKEQQ	GAGTTCTCTAAGAACACAG			
		Mouse	EFSKEQQ	GAGTTCTCTAAGGAGCAACAG			
		Pig	EFSKEQQ	GAGTTCTCTAAGAACACAG			
		Dolphin	EFSQOOQ	GAGTTCTCTCAGAACACAG	A → C		
		Cow	EFSQOOQ	GAGTTCTCTAAGAACACAG			
		Megabat	QFSKEQQ	CAGTTCTCTAAGAACACAG			
		Microbat	EFSQEOQ	GAGTTCTCTCAGAACACAG	A → C		
Total number							
G/C → C/G or A/T → T/A					5		
G/C → A/T					8		
A/T → G/C					4		

Table S5. Top 30 genes with a significantly higher expression level in the anterior cricothyroid muscle compared to breast muscle of *P. parnellii*.

Parvalbumin, which temporarily binds Ca²⁺ in the sarcoplasm of superfast muscles (32), is the third-ranked gene. It is also noteworthy that the gene with the highest log fold change, *RYR3*, has a parallel substitution (V2739I) of conservative nature in a highly-conserved alignment position that occurs only in the echolocating bat and dolphin.

Gene symbol	Gene name	normalized read counts						average expression		log fold change adjusted P-value			
		anterior cricothyroid muscle (ACTM)			breast muscle								
		sample 1	sample 2	sample 3	sample 1	sample 2	sample 3	ACTM	breast				
<i>RYR3</i>	ryanodine receptor 3	30.53	26.65	22.91	0.02	0.16	0.06	26.70	0.08	7.7	1.4E-77		
<i>MEIS2</i>	Meis homeobox 2	14.20	13.19	10.16	0.26	0.19	0.15	12.52	0.20	5.5	8.6E-50		
<i>PVALB</i>	parvalbumin	875.68	1002.8	965.13	3.78	5.11	14.78	947.88	7.89	6.2	8.4E-48		
<i>NPPA</i>	natriuretic peptide A	25.66	22.02	17.93	0.00	0.23	0.09	21.87	0.11	6.9	7.9E-46		
<i>CNTFR</i>	ciliary neurotrophic factor receptor	35.55	37.21	27.63	0.52	1.20	1.40	33.46	1.04	4.5	8.3E-38		
<i>ZNF385A</i>	zinc finger protein 385A	29.06	37.25	24.30	0.09	0.66	0.15	30.20	0.30	5.9	2.4E-35		
<i>TMEM229B</i>	transmembrane protein 229B	14.15	6.17	7.63	0.05	0.08	0.02	9.32	0.05	6.5	5.7E-32		
<i>PITX1</i>	paired-like homeodomain 1	16.65	15.21	9.84	0.03	0.24	0.21	13.90	0.16	5.6	1.0E-31		
<i>ADGB</i>	androglobin	6.14	11.01	9.82	0.00	0.07	0.04	8.99	0.03	6.7	6.2E-28		
<i>SERPINA3</i>	serpin family A member 3	15.87	9.63	5.22	0.00	0.09	0.00	10.24	0.03	7.2	1.3E-25		
<i>CDO1</i>	cysteine dioxygenase type 1	19.52	30.61	31.31	1.88	1.50	2.25	27.14	1.88	3.8	6.7E-25		
<i>ZNF385B</i>	zinc finger protein 385B	5.74	4.26	3.70	0.08	0.13	0.01	4.57	0.07	5.3	4.3E-23		
<i>SH3RF2</i>	SH3 domain containing ring finger 2	7.15	2.92	2.49	0.16	0.02	0.06	4.19	0.08	5.1	1.1E-22		
<i>MPZ</i>	myelin protein zero	17.27	25.01	16.37	1.20	0.60	0.54	19.55	0.78	4.0	5.6E-22		
<i>AUTS2</i>	autism susceptibility candidate 2	22.07	7.63	4.21	0.17	0.34	0.09	11.30	0.20	5.1	1.3E-21		
<i>TSHZ2</i>	teashirt zinc finger homeobox 2	3.06	3.81	4.01	0.38	0.36	0.41	3.63	0.38	2.9	2.2E-21		
<i>ERBB3</i>	erb-b2 receptor tyrosine kinase 3	1.64	1.75	1.83	0.06	0.08	0.05	1.74	0.06	4.4	2.8E-21		
<i>SLC4A3</i>	solute carrier family 4 member 3	4.91	4.10	4.14	0.03	0.08	0.02	4.38	0.04	5.6	2.9E-21		
<i>FRMD3</i>	FERM domain containing 3	15.86	23.70	23.66	0.00	0.31	0.00	21.07	0.10	6.3	3.2E-21		
<i>ANKRD50</i>	ankyrin repeat domain 50	4.88	3.57	4.58	0.44	0.64	0.48	4.34	0.52	2.7	7.3E-21		
<i>SHOX</i>	short stature homeobox	6.90	4.23	2.56	0.00	0.00	0.00	4.56	0.00	7.2	1.9E-20		
<i>PTPRS</i>	protein tyrosine phosphatase, receptor type S	4.42	5.12	4.54	0.52	0.86	0.56	4.69	0.65	2.6	4.0E-20		
<i>GNAI2</i>	G protein subunit alpha i2	2.48	2.46	3.01	0.11	0.23	0.18	2.65	0.17	3.7	1.5E-19		
<i>BARX2</i>	BARX homeobox 2	6.70	12.26	9.11	0.12	0.29	0.59	9.36	0.33	4.1	1.1E-18		
<i>ADAMTSL4</i>	ADAMTS like 4	6.47	8.81	7.39	0.62	0.96	0.39	7.56	0.66	3.0	1.7E-18		
<i>ATP11A</i>	ATPase phospholipid transporting 11A	5.99	6.06	7.28	0.89	0.98	0.85	6.44	0.91	2.4	5.3E-18		
<i>SLC1A5</i>	solute carrier family 1 member 5	4.21	4.17	3.16	0.43	0.30	0.53	3.84	0.42	2.8	4.8E-17		
<i>SPHKAP</i>	SPHK1 interactor, AKAP domain containing	1.67	1.92	1.64	0.09	0.10	0.08	1.74	0.09	4.3	5.4E-17		
<i>CTXN3</i>	cortexin 3	39.17	37.48	30.79	0.21	1.45	1.82	35.81	1.16	4.2	6.2E-17		
<i>ITGB4</i>	integrin subunit beta 4	3.65	4.23	3.36	0.18	0.53	0.25	3.75	0.32	3.1	1.3E-16		

Table S6. Expression of calsequestrin, Ca²⁺ ATPase, myosin heavy chain, and myosin light chain genes in the anterior cricothyroid muscle and the breast muscle of the echolocating *P. parnellii* bat.

The top part lists the normalized read counts obtained for three biological replicates (data is also shown in Fig. 4 main text). The bottom part lists the median read count ratios between fast-twitch and slow-twitch fiber genes and the statistical significance computed by a two-sided unequal variances t-test that is implemented in R.

Gene	anterior cricothyroid muscle (ACTM)			breast muscle		
	normalized read counts					
	biological replicate 1	biological replicate 2	biological replicate 3	biological replicate 1	biological replicate 2	biological replicate 3
CASQ1	236.99	297.95	197.45	113.59	402.07	348.41
CASQ2	35.62	26.71	16.52	34.41	69.82	73.88
ATP2A1	2766.67	2078.00	1835.32	579.84	1087.72	1153.78
ATP2A2	2.35	2.39	3.33	466.78	169.37	90.33
MYH4	4649.28	2688.12	2770.09	348.76	502.85	978.52
MYH2	442.69	353.66	240.77	727.28	3408.00	1942.28
MYH1	35.54	50.40	30.12	1567.41	2053.80	3399.88
MYH6	0.21	0.29	0.59	2090.40	873.83	414.74
MYL1	517.75	501.36	506.47	383.36	1023.16	908.16
MYL3	0.00	0.05	0.10	376.32	196.78	61.33
statistics						
CASQ1 vs. CASQ2	t value, df	P-value	median ratio	t value, df	P-value	median ratio
CASQ1 vs. CASQ2	7.32, 2.1	0.01498	8.87	2.56, 2.1	0.1203	4.99
ATP2A1 vs. ATP2A2	7.97, 2.0	0.01537	868.37	3.26, 3.4	0.0399	6.42
MYH4 vs. MYH6	5.26, 2.0	0.03430	9552.05	-0.97, 2.6	0.4163	0.58
MYH2 vs. MYH6	5.91, 2.0	0.02745	1219.52	0.98, 3.4	0.3932	2.22
MYH1 vs. MYH6	6.32, 2.0	0.02409	122.54	1.64, 4.0	0.1777	2.35
MYL1 vs. MYL3	104.98, 2.0	0.00009	10551.42	2.58, 2.8	0.0870	4.61